Internal Medicine
The Japanese Society of Internal Medicine
doi: 10.2169/internalmedicine.3831-19
Intern Med 59: 663-671, 2020
http://internmed.jp

【 CASE REPORT 】

Predominant Involvement of the Aortic Root in a Patient with Anti-neutrophil Cytoplasmic Antibody-associated Vasculitis: Congestive Heart Failure due to Subacute Severe Aortic Regurgitation and Reversible Conduction Disturbance

Atsusuke Yatomi[1], Shumpei Mori[1], Hirotaka Kawauchi[1], Ayu Shono[1], Shinsuke Shimoyama[2], Hidekazu Tanaka[1], Takaichi Okano[3], Takeshi Inoue[4], Naoe Jimbo[5], Akio Morinobu[3] and Ken-ichi Hirata[1]

Abstract:

A 72-year-old woman was referred to our institution with decompensated congestive heart failure owing to subacute severe aortic regurgitation and mitral regurgitation. Her blood sample tested positive for myeloperoxidase anti-neutrophil cytoplasmic antibody (ANCA). Cardiac computed tomography revealed abnormal thickening and shortening of the aortic valvar leaflets as well as wall thickening of the sinuses of Valsalva. Based on the diagnosis of ANCA-associated vasculitis, predominantly involving the aortic root, prednisolone administration was initiated, which failed to improve the valvar dysfunction. The patient underwent aortic root replacement and mitral annuloplasty. Histopathology confirmed severe inflammation involving both the aortic valvar sinuses and leaflets.

Key words: ANCA-associated vasculitis, aortic regurgitation, aortic root, conduction disturbance, congestive heart failure

(Intern Med 59: 663-671, 2020)
(DOI: 10.2169/internalmedicine.3831-19)

Introduction

Vasculitis is inflammation of the blood vessel walls. It is often categorized based on the size of the vessels predominantly involved; for example, anti-neutrophil cytoplasmic antibody (ANCA)-associated vasculitis (vasculitis of small vessels), Kawasaki disease (vasculitis of medium-sized vessels), and Takayasu arteritis (vasculitis of large vessels). Differences among these categories of vessels correlate with the function and susceptibility to specific variants of vasculitis (1). ANCA-associated vasculitis predominantly affects the small vessels (1, 2).

However, we herein report a patient with ANCA-associated vasculitis predominantly involving the aortic root that demonstrated conduction disturbance and congestive heart failure due to subacute severe aortic regurgitation.

Case Report

A 72-year-old woman with a history of limited cutaneous systemic sclerosis was referred to our institution because of decompensated congestive heart failure. She manifested general fatigue, palpitation, and weight loss during the previous

[1]Division of Cardiovascular Medicine, Department of Internal Medicine, Kobe University Graduate School of Medicine, Japan, [2]Department of Radiology, Kobe University Graduate School of Medicine, Japan, [3]Department of Rheumatology and Clinical Immunology, Kobe University Graduate School of Medicine, Japan, [4]Department of Cardiovascular Surgery, Kobe University Graduate School of Medicine, Japan and [5]Department of Diagnostic Pathology, Kobe University Graduate School of Medicine, Japan
Received: August 22, 2019; Accepted: September 26, 2019; Advance Publication by J-STAGE: November 8, 2019
Correspondence to Dr. Shumpei Mori, shumpei_8@hotmail.com

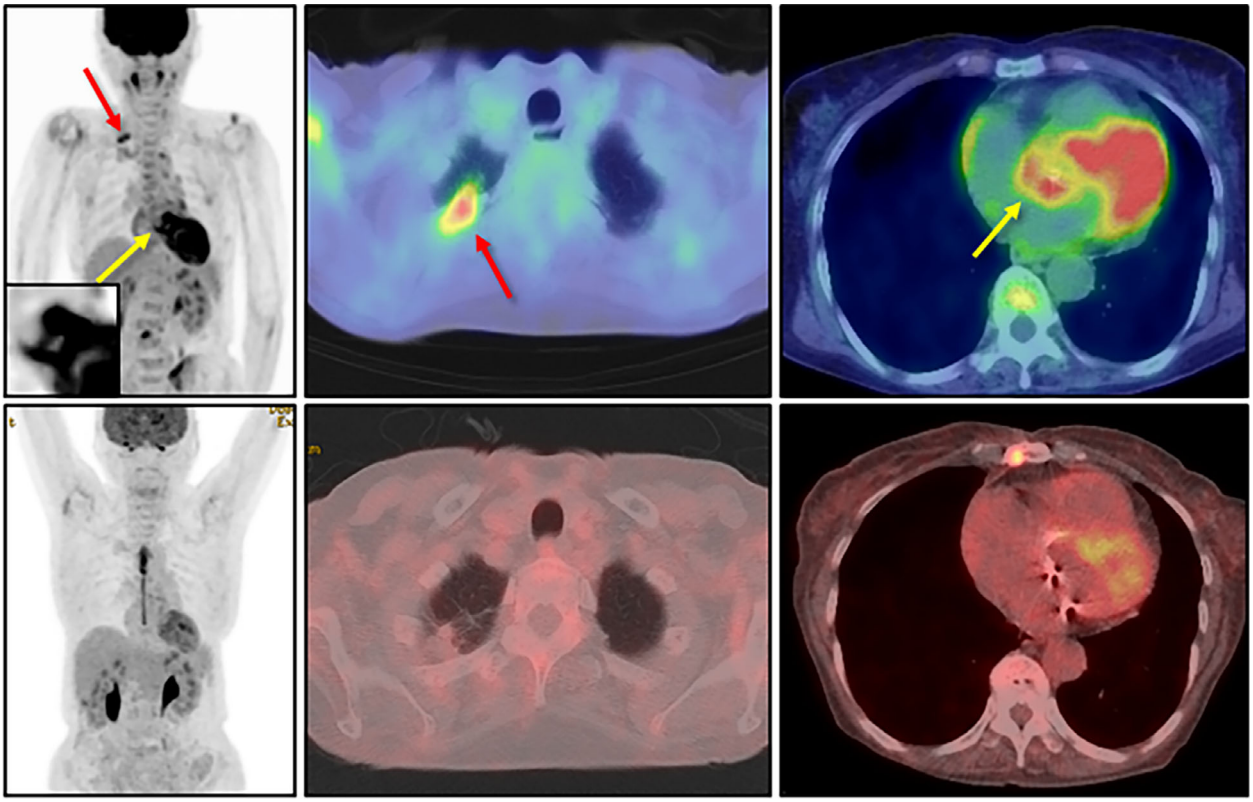

Figure 1. Pre- and post-operative findings of ^{18}F-fluorodeoxyglucose positron emission tomography/computed tomography. Before the immunosuppressive therapy (upper panels), an intense accumulation was detected at the apex of the right lung (red arrows) as well as the aortic root (yellow arrows). Since long-term fasting had not been performed for this study, the myocardial accumulation itself was considered a potentially physiological finding. The aortic root is magnified in the inset. After immunosuppressive therapy (lower panels) performed under 18-hour fasting with heparin injection, the disappearance of both abnormal accumulations was confirmed.

three months.

During a thorough examination at the previous hospital, a dense nodule was detected at the apex of the right lung, and it was positive on ^{18}F-fluorodeoxyglucose positron emission tomography/computed tomography (Fig. 1). Since long-term fasting had not been performed for this study, the myocardial accumulation itself was considered a physiological finding. The intense and abnormal accumulation at the aortic root, however, was also detected (Fig. 1). In addition, myeloperoxidase (MPO)-ANCA and anti-centromere antibodies were also positive.

Transthoracic echocardiography detected moderate aortic regurgitation and mild mitral regurgitation. Although a transbronchial lung biopsy was scheduled, it was cancelled because of dyspnea at rest and orthopnea within two weeks before her consultation with our hospital. As repeated transthoracic echocardiography confirmed subacute progression of the aortic and mitral regurgitation to a severe degree, she was transferred to our hospital for multidisciplinary management. Right heart catheterization performed immediately before the transfer revealed decompensated heart failure, classified as Forrester IV, as follows: pulmonary artery wedge pressure a24/v42/m26 mmHg, pulmonary artery pressure s61/d24/m39 mmHg, right ventricular pressure s56/b3/e8 mmHg, right atrial pressure a10/v4/m5 mmHg, and a cardiac index of 1.99 L/min/m^2.

On admission, her blood pressure was 116/42 mmHg, with a regular pulse heart rate of 92 beats per minute. She was afebrile, and her oxygen saturation was 98% on 2 L/min of oxygen. Auscultation revealed a third heart sound, a to-and-fro murmur in the third intercostal space at the left sternal border, and a systolic regurgitant murmur at the apex. Quincke's pulse was also noticed. A physical examination finding consistent with limited cutaneous systemic sclerosis was restricted to her fingers. No findings showing granulomatous vasculitis affecting the eyes, nose, or ears were revealed on a thorough examination by an otorhinolaryngologist.

Initial blood tests showed marked inflammation and elevated serum liver enzymes, troponin I, and brain natriuretic peptide levels (Table 1). Furthermore, positivity for MPO-ANCA (164.3 U/mL) as well as anti-centromere antibody was confirmed (Table 2). A urinalysis revealed positive occult blood (Table 1). Chest radiography showed dilation of the cardiac silhouette, with pulmonary congestion. An electrocardiogram demonstrated complete right bundle branch

Table 1. Laboratory Data on Admission 1.

Peripheral blood		Aspartate aminotransferase	35 IU/L
White blood cells	14,500 /μL	Alanine aminotransferase	37 IU/L
Neutrophils	87.0 %	Gamma-glutamyl transpeptidase	83 IU/L
Eosinophils	4.0 %	Alanine transaminase	462 IU/L
Monocytes	2.0 %	Lactate dehydrogenase	243 IU/L
Lymphocytes	7.0 %	Creatine kinase	38 IU/L
Red blood cells	332×10^4 /μL	Creatine kinase MB	<4 IU/L
Hemoglobin	9.1 g/dL	Troponin I	2.49 ng/mL
Platelets	41.0×10^4 /μL	Brain natriuretic peptide	762 pg/mL
		Hemoglobin A1c	6.8 %
Coagulation		C-reactive protein	3.34 mg/dL
Activated partial thromboplastin time	27.3 sec		
Prothrombin time	85.3 %	Tumor maker	
Fibrinogen	575 mg/dL	Squamous cell carcinoma antigen	0.7 ng/mL (<1.5)
D-dimer	6.5 μg/dL	Sialyl-Lewis^x antigen	25.7 U/mL (0-38)
		Pro-gastrin-releasing peptide	39.6 pg/mL (<81)
Biochemistry			
Sodium	137 mEq/L	Urinalysis	
Potassium	4.1 mEq/L	Specific gravity	1.016
Chloride	100 mEq/L	Potential of hydrogen	6.5
Calcium	8.7 mg/dL	Protein	None
Phosphorus	3.4 mg/dL	Glucose	None
Blood urea nitrogen	16.9 mg/dL	Ketones	None
Serum creatinine	0.62 mg/dL	Occult blood	1+
Estimated glomerular filtration rate	70.9 mL/min/1.73m^2	Urobilinogen	1+
Total protein	6.3 g/dL	Red blood cells	49 /μL
Serum albumin	2.2 g/dL	White blood cells	21 /μL
Total bilirubin	0.9 mg/dL	Bacteria	1+

Numbers in parentheses indicate normal range.

block with progressive left axis deviation and a prolonged PR interval compared to a recording at the previous hospital. These findings indicated exacerbated trifascicular block (Fig. 2). Transthoracic echocardiography showed a preserved systolic left ventricular function (ejection fraction of 60%) without left ventricular dilatation (end-diastolic dimension of 51 mm), massive aortic regurgitation with thickened and shortened valvar leaflets predominantly affecting the left coronary aortic leaflet, and severe functional mitral regurgitation due to annular dilatation (Fig. 3).

To evaluate the anatomy of the aortic root and the aortic valve as well as of the coronary arteries, electrocardiographically-gated contrast-enhanced computed tomography was performed, using a third-generation dual-source computed tomographic scanner (SOMATOM Force; Siemens Healthcare, Forchheim, Germany). Both coronary arteries were intact. All three aortic valvar leaflets were thickened and shortened, with a significant coaptation gap. Wall thickening of the sinuses of Valsalva was also observed. The virtual basal ring plane showed abnormal thickening of the area of aortic-to-mitral continuity (Fig. 4).

Based on these clinical features, the diagnosis of ANCA-associated vasculitis (microscopic polyangiitis) (3, 4), predominantly involving the aortic root, was then confirmed. A lung nodule biopsy was avoided, as her hemodynamic status was rapidly being exacerbated. As progressive worsening of the conduction disturbance was considered to have been induced by inflammation involving the atrioventricular conduction axis and proximal left and right bundle branches, located right beneath the aortic root (Fig. 1, 2, 4), we promptly initiated treatment with glucocorticoids. This decision was made because the further deterioration of her hemodynamic status due to the development of complete atrioventricular block risked a catastrophic outcome that could not easily be rescued using percutaneous cardiopulmonary support and/or an intra-aortic balloon pump, as the patient showed severe aortic regurgitation.

On the fifth day of hospitalization, the daily administration of oral prednisolone 45 mg (1 mg/kg) was initiated. Fortunately, along with the rapid improvement in inflammation and the serum Troponin I level (Fig. 5), conduction disturbances also promptly showed a tendency to improve (Fig. 2, 5). However, contrary to our expectations, severe aortic and mitral regurgitations showed no signs of improvement; in fact, her heart failure rapidly worsened and required inotropic support and noninvasive positive pressure ventilation (Fig. 5). Paroxysmal atrial fibrillation developed as well. On the 12th day of hospitalization, the patient underwent an emergent Bentall operation with a bioprosthetic aortic valve, mitral annuloplasty, Maze procedure, and left

Table 2. Laboratory Data on Admission 2.

Immunological		
Immunoglobulin G	1,133	mg/dL
Immunoglobulin A	329	mg/dL
Immunoglobulin M	84	mg/dL
Complement C3	112	mg/dL (73-138)
Complement C4	35	mg/dL (11-31)
Complement C1q	<1.5	/μL
Anti-nuclear antibody	1:1280	(Centromere pattern) (<40)
Anti-double-stranded deoxyribonucleic acid antibody	1.7	IU/mL (0-12.0)
Anti-single-stranded deoxyribonucleic acid antibody	1.9	AU/mL (0-25.0)
Anti-Sm antibody	0.2	U/mL (0-9.9)
Anti-Sjögren's-syndrome-related antigen A	0.5	U/mL (0-9.9)
Anti-Sjögren's-syndrome-related antigen B	0.5	U/mL (0-9.9)
Anti-Scl-70 antibody	<5	U/mL (<16)
Anti-centromere antibody	128	U/mL (<10)
Anti-Mi-2 antibody	<5	(<53)
Anti-aminoacyl-tRNA synthetase antibody	<5	(<25)
Anti-melanoma differentiation-associated gene 5 antibody	5	(<32)
Rheumatoid factor	118	IU/mL (<15)
Anti-cyclic citrullinated peptide antibody	0.5	U/mL (<4.5)
Myeloperoxidase anti-neutrophil cytoplasmic antibody	164.3	U/mL (<3.5)
Proteinase 3 anti-neutrophil cytoplasmic antibody	4.1	U/mL (<3.5)
Antimitochondrial antibody	<20	(<20)
Soluble interleukin-2 receptor	825	U/mL (121-613)
Tuberculosis interferon gamma release assay (T-SPOT.TB)	negative	
Anti-glycopeptidolipid-core IgA antibody	<0.5	U/mL (<0.7)

Numbers in parentheses indicate normal range. tRNA: transfer ribonucleic acid

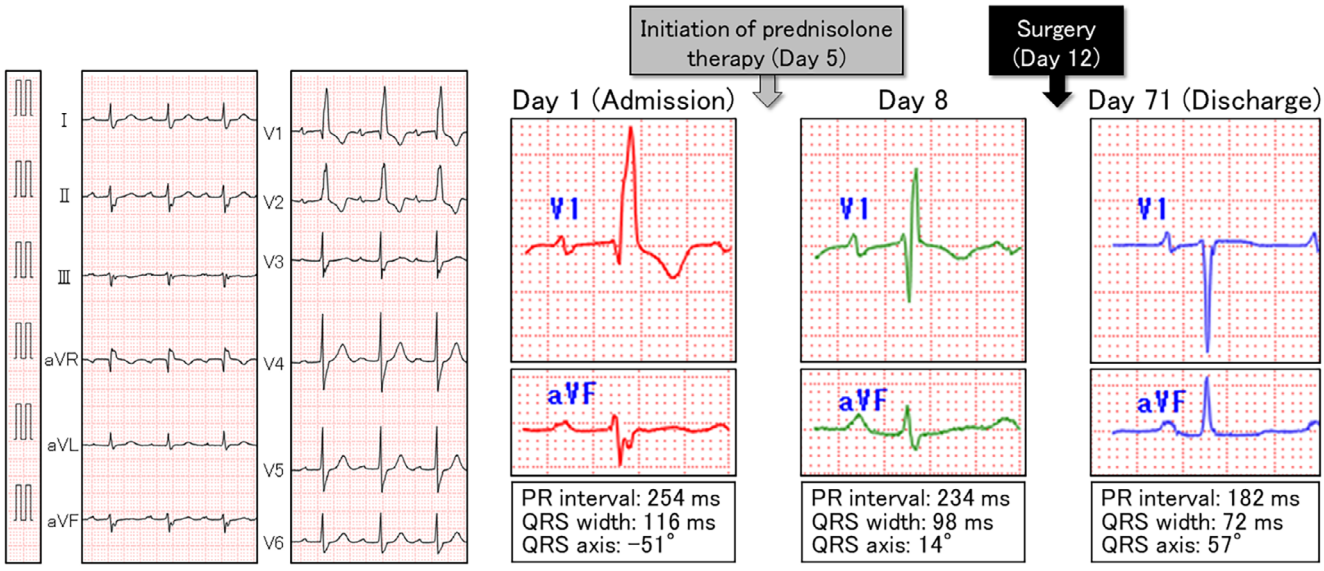

Figure 2. Electrocardiogram on admission and its temporal course. On admission (left panels), trifascicular block was observed. Just three days after the initiation of prednisolone therapy (right panels), prompt improvements in the PR interval, QRS width, and QRS axis were observed. At discharge, the PR interval, QRS width, and QRS axis recovered to the normal range.

atrial appendage occlusion. During surgery, severe degeneration (thickening, shortening, and whitish change due to fibrosis) of the aortic valve as well as the sinuses of Valsalva was confirmed (Fig. 6). Conversely, the mitral valve showed no organic degeneration indicating valvar inflammation. Mitral regurgitation, therefore, was controlled with mitral annuloplasty alone.

Histopathology demonstrated predominant and diffuse in-

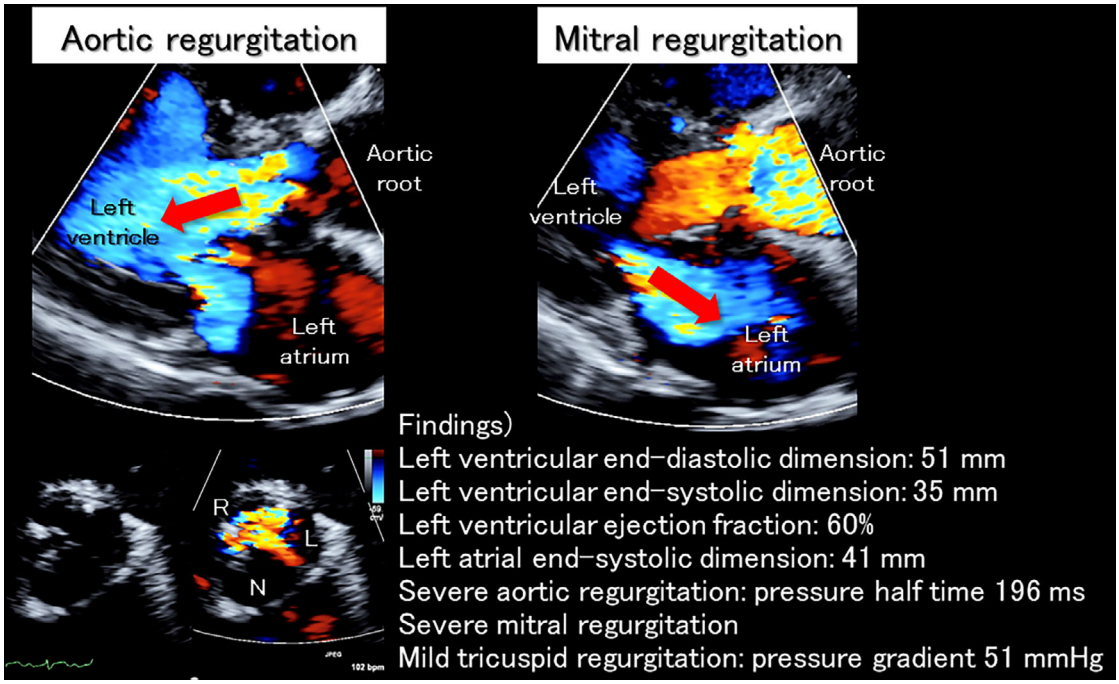

Figure 3. **Echocardiographic findings on admission. On admission, massive aortic regurgitation (red arrow in the left upper panel) was noted. The left coronary aortic leaflet almost lost its mobility due to thickening and shortening, creating a significant gap between the other two leaflets (left lower panels), which can be seen as the wide vena contracta in the parasternal long axis view (left upper panel). Severe functional mitral regurgitation (red arrow in the right panel) due to mitral annular dilatation was also noted. L: left coronary aortic leaflet; N: non-coronary aortic leaflet; R: right coronary aortic leaflet**

filtration of CD8+ T-lymphocytes into the fibrosa of the aortic valvar leaflets. Furthermore, inflammatory cells (CD8+ T-lymphocytes, CD20+ B-lymphocytes, and CD68+ multinucleated giant cells) intensively infiltrated the adventitia of the sinuses of Valsalva, predominantly around the vasa vasorum (Fig. 7).

After surgery, her heart failure improved, and the prednisolone dose was able to be tapered. One month postoperatively, additional remission induction therapy was withheld to avoid postoperative complications, including mediastinal infection and surgical wound dehiscence. One month later, four courses of rituximab therapy for ANCA-associated vasculitis were additionally initiated (Fig. 5) before discharge. Follow-up ^{18}F-fluorodeoxyglucose positron emission tomography/computed tomography performed under 18 hours of fasting with heparin injection clearly demonstrated improvement in the abnormal accumulation involving the aortic root and right apical lung (Fig. 1). However, while the abnormal accumulation disappeared, the size of the lung nodule did not show any significant changes through the clinical course. We decided not to perform a biopsy of this lesion, and it was followed by scheduled computed tomography. At that point, whether or not this lesion was ANCA-associated vasculitis granuloma was unclear. The MPO-ANCA serum level decreased to the normal range (2.2 U/mL) after an additional 4 courses of rituximab treatment. Positive occult blood on a urinalysis also disappeared. She remains event-free and asymptomatic at eight months after discharge.

Discussion

We encountered a case of ANCA-associated vasculitis predominantly involving the aortic root, combined with conduction disturbance. Following the prompt administration of glucocorticoids that, we believe, successfully prevented a catastrophe due to complete atrioventricular block, emergent radical surgery for valvar regurgitation was performed, which saved her life.

Although the role of ANCA in the pathogenesis of vasculitis has not been fully elucidated, ANCA-associated vasculitis is classified as necrotizing vasculitis predominantly affecting small vessels (1, 2). The ANCA titer is considered to reflect the disease activity (3), as observed in this patient (Fig. 5). ANCA-associated vasculitis affecting the aorta and its major branches, heart valves, and the cardiac conduction system has been reported (5-10). Involvement of the heart valves and conduction systems is more frequently reported in patients with granulomatosis with polyangiitis (5, 7-10) associated with proteinase 3-ANCA than in those with microscopic polyangiitis associated with MPO-ANCA. Nakabayashi et al. (6) suspected that MPO-ANCA induces small vessel vasculitis, which occurs in the vasa vasorum of large arteries; vasa vasorum vasculitis results in the pathological process of aortitis. Although the histopathological findings

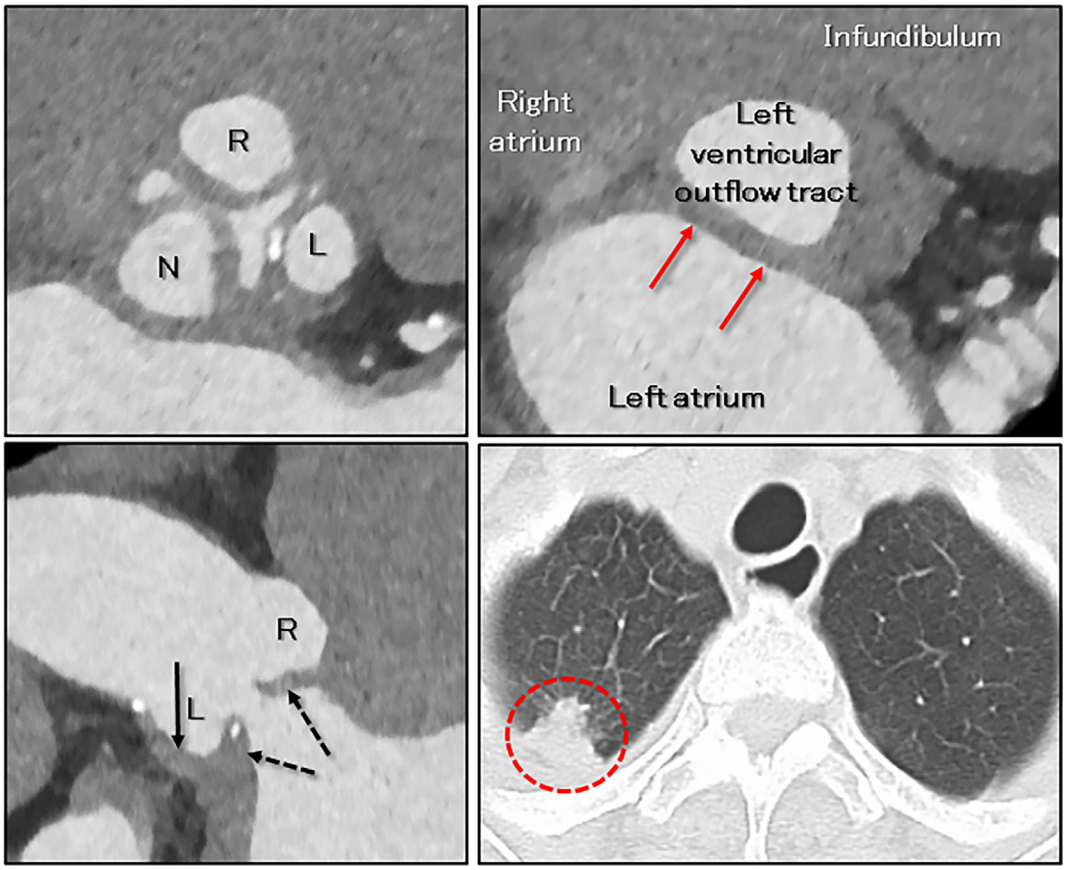

Figure 4. **Cardiac computed tomographic findings on admission (mid-diastole reconstruction). The aortic valvar leaflets were thickened and shortened, which was predominant in the left coronary aortic leaflet (left upper panel, dashed arrows in the left lower panel), with a significant coaptation gap (regurgitant orifice) in mid-diastole (left panels). Abnormal thickening of the wall of the sinuses of Valsalva (arrow in the left lower panel) and the aortic-to-mitral continuity (red arrows in the right upper panel show the virtual basal ring plane) were also detected. The red dashed circle in the right lower panel shows a nodule at the apex of the right lung (Fig. 1). L: left coronary aortic leaflet; N: non-coronary aortic leaflet; R: right coronary aortic leaflet**

of the present patient were affected by the preceding administration of prednisolone, predominant inflammatory cell infiltration around the vasa vasorum at the adventitia supports the speculation concerning the mechanism of ANCA-associated vasculitis involving large vessels.

Among 77 patients with systemic sclerosis, 7 (9.1%) were MPO-ANCA-positive by both an immunofluorescence test and enzyme-linked immunosorbent assay (11). Why ANCA-associated vasculitis occurs in systemic sclerosis is unknown at present. A meta-analysis focusing on 50 ANCA-positive patients with systemic sclerosis with an average age of 57.1 ±11.9 years, female (42 patients, 84%) and MPO-ANCA (36 patients, 72%) predominance were reported (12). Anti-topoisomerase I (anti-Scl-70) antibody was the predominant systemic sclerosis-associated antibody (35 patients, 70%), followed by the anti-centromere antibody (7 patients, 14%). The anti-topoisomerase I antibody was a risk factor for developing ANCA-associated vasculitis in this patient cohort (12), a finding that is discrepant with the observation in our patient, who was negative for anti-Scl-70 antibody (Table 2).

Dual immunosuppression therapy including glucocorticoids and cyclophosphamide/rituximab is commonly selected for remission induction therapy (2). We selected rituximab for this patient, considering the potential cardiotoxicity of cyclophosphamide. Of note, the infiltration of CD20+ cells was confirmed in the histopathological specimen examination (Fig. 7). Concerning the perioperative complications induced by dual immunosuppression therapy, we first administered glucocorticoid only, without rituximab. At one month after surgery, following a sufficient period of wound healing without infection, we added rituximab. This individualized strategy was almost certainly effective in preventing catastrophic consequences of complete atrioventricular block in this patient, avoiding perioperative pacemaker implantation and preventing perioperative complications. Since there is no guideline concerning this particular situation, we based our strategy on clinical judgement through a multidisciplinary discussion. During the discussion, we concluded that emergent surgery during active surgical site inflammation or with dual immunosuppression therapy should be avoided.

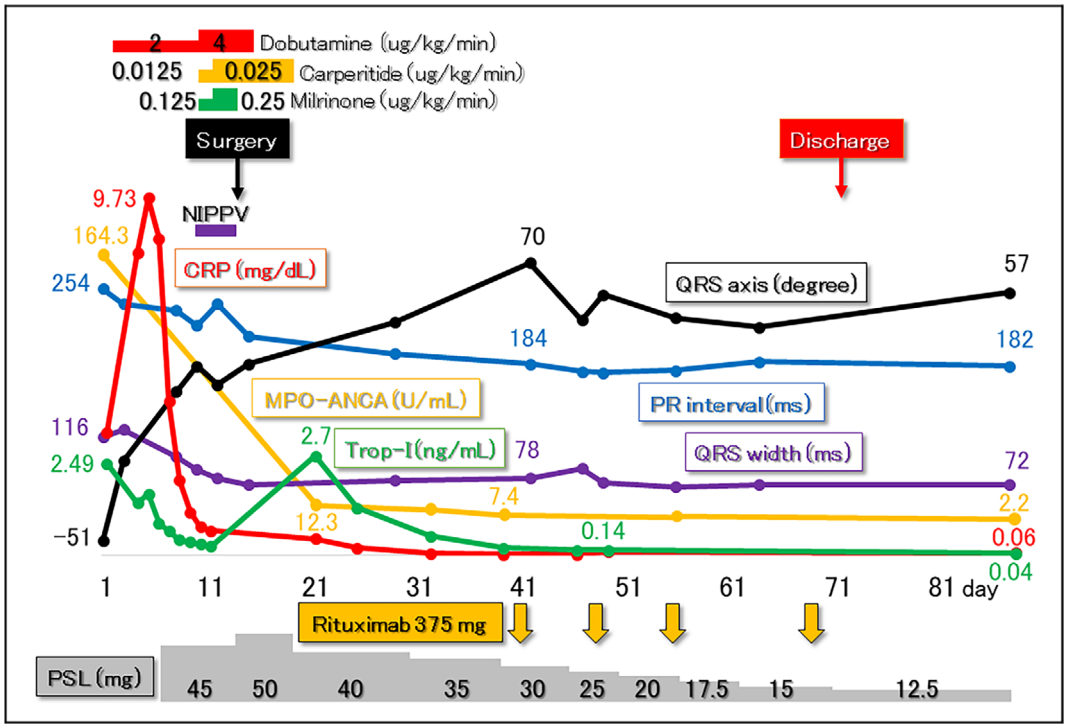

Figure 5. **Clinical course after admission. Following the diagnosis of myeloperoxidase (MPO) anti-neutrophil cytoplasmic antibody (ANCA) -associated vasculitis, administration of prednisolone (PSL) was initiated (day 5). Along with prompt improvement in the values of C-reactive protein (CRP) and serum troponin I (Trop-I), conduction disturbances started to recover before surgery. However, congestive heart failure due to severe aortic and mitral regurgitation showed no signs of improvement, requiring inotropic support and noninvasive positive pressure ventilation (NIPPV). Emergent curative surgery, including a Bentall operation and mitral annuloplasty, was therefore performed on day 12. The clinical course after surgery was uneventful. Along with the temporary decrease in the prednisolone dose, additional remission induction therapy with four courses of rituximab was initiated (orange arrows).**

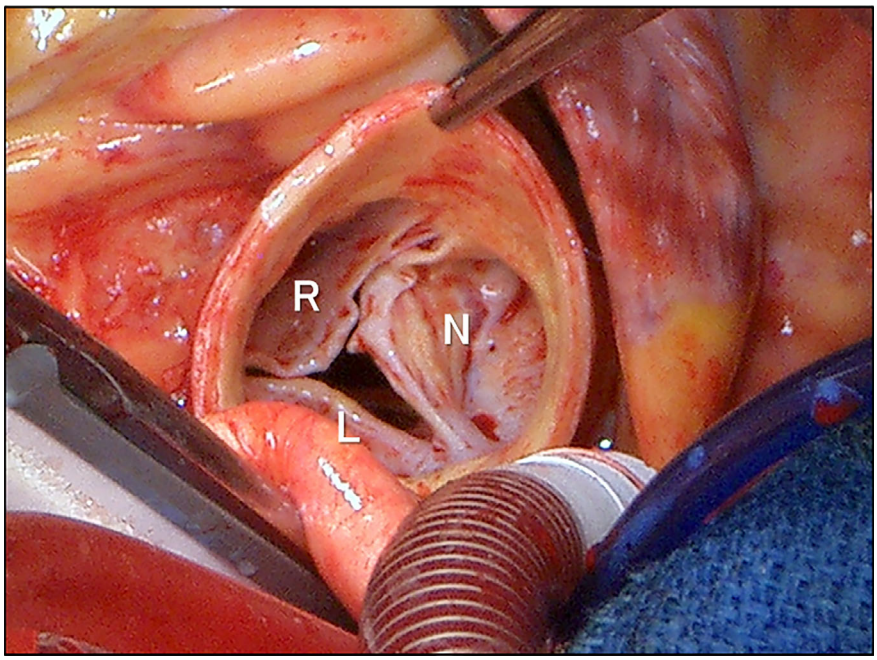

Figure 6. **Surgical findings during operation. Severe degeneration (thickening, shortening, and whitish changes due to fibrosis) of the aortic valve, which was prominent in the left coronary aortic leaflet, and the wall of the sinuses of Valsalva was directly confirmed. Refer to Figures 3 and 4. L: left coronary aortic leaflet, N: non-coronary aortic leaflet, R: right coronary aortic leaflet**

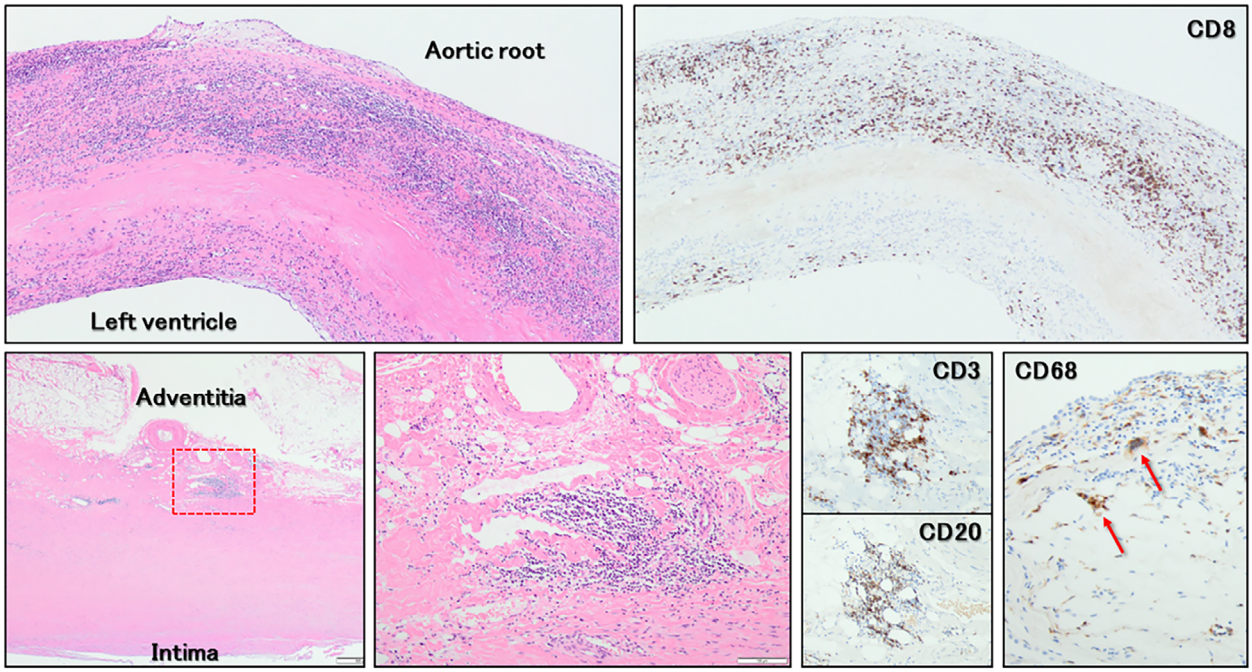

Figure 7. **Histopathological findings (Hematoxylin and Eosin staining and immunostaining). Predominant and diffuse infiltration of CD8+ T-lymphocytes into the fibrosa of the aortic valvar leaflet (upper panels) is observed. On the adventitia of the sinuses of Valsalva (lower panels), CD8+ T-lymphocytes, CD20+ B-lymphocytes, and CD68+ multinucleated giant cells (red arrows) infiltrated predominantly around the vasa vasorum. The lower middle panel shows a magnified view of the red dashed box in the lower left panel.**

Contrast-enhanced computed tomography is useful for detecting vasculitis involving large and medium-sized vessels as wall thickening and/or stenotic lesions (13, 14). We showed that electrocardiographically gated cardiac computed tomography is also effective for assessing the aortic root and heart valves without motion artifacts. In the present case, abnormal thickening of the aortic valve as well as of the wall of the sinuses of Valsalva (Fig. 4) suggested that this was a case of vasculitis predominantly confined to the aortic root. Furthermore, abnormal thickening of the aortic-to-mitral continuity showed that the inflammation was propagating beneath the aortic valve toward the left ventricular outflow tract. This observation warned us of the risk of complete atrioventricular block development, as the proximal part of the atrioventricular conduction is closely associated with the membranous septum, which is located at the septal part of the left ventricular outflow tract (15). Although an endomyocardial biopsy was not performed during surgery, the elevated serum Troponin I levels at admission and their prompt improvement after the administration of prednisolone despite the rapid exacerbation of congestive heart failure supported a diagnosis of myocardial inflammation involving the left ventricular outflow tract owing to ANCA-associated vasculitis.

In conclusion, we treated a patient with ANCA-associated vasculitis predominantly involving the aortic root. Individualized immunosuppression therapy based on a multidisciplinary approach and multimodality imaging ensured successful patient management without complications. We believe it is clinically important to share our challenging experience in order to guide the treatment of patients with similar comorbidities.

The authors state that they have no Conflict of Interest (COI).

References

1. Jennette JC, Falk RJ, Bacon PA, et al. 2012 revised international chapel hill consensus conference nomenclature of vasculitides. Arthritis Rheum **65**: 1-11, 2013.
2. 2017 Japanese guideline for management of ANCA-associated vasculitis [Internet]. [cited 2019 Jul 28]. Available from: https://minds.jcqhc.or.jp/docs/minds/ANCA-associated-vasculitis/ANCA-associated-vasculitis.pdf (in Japanese)
3. Japan Intractable Disease Information Center [Internet]. [cited 2019 Jul 28]. Available from: http://www.nanbyou.or.jp/entry/245 (in Japanese)
4. Watts R, Lane S, Hanslik T, et al. Development and validation of a consensus methodology for the classification of the ANCA-associated vasculitides and polyarteritis nodosa for epidemiological studies. Ann Rheum Dis **66**: 222-227, 2007.
5. Forstot JZ, Overlie PA, Neufeld GK, Harmon CE, Forstot SL. Cardiac complications of Wegener granulomatosis: a case report of complete heart block and review of the literature. Semin Arthritis Rheum **10**: 148-154, 1980.
6. Nakabayashi K, Kamiya Y, Nagasawa T. Aortitis syndrome associated with positive perinuclear antineutrophil cytoplasmic antibody: report of three cases. Int J Cardiol **75**: S89-S94, 2000.
7. Suleymenlar G, Sarikaya M, Sari R, Tuncer M, Sevinc A. Com-

plete heart block in a patient with Wegener's granulomatosis in remission-a case report. Angiology **53**: 337-340, 2002.

8. Yahalom M, Roguin N, Antonelli D, Suleiman K, Turgeman Y. Association of heart block with uncommon disease States. Int J Angiol **22**: 171-176, 2013.

9. Colin GC, Vancraeynest D, Hoton D, et al. Complete heart block caused by diffuse pseudotumoral cardiac involvement in granulomatosis with polyangiitis. Circulation **132**: e207-e210, 2015.

10. Taskesen T, Goldberg SL, Mannelli L, et al. Granulomatosis with polyangiitis presenting with an intracardiac mass and complete heart block: enhanced images by 3-dimensional echocardiography. Circulation **132**: 961-964, 2015.

11. Akimoto S, Ishikawa O, Tamura T, Miyachi Y. Antineutrophil cytoplasmic autoantibodies in patients with systemic sclerosis. Br J Dermatol **134**: 407-410, 1996.

12. Rho YH, Choi SJ, Lee YH, Ji JD, Song GG. Scleroderma associated with ANCA-associated vasculitis. Rheumatol Int **26**: 369-375, 2006.

13. Martinez F, Chung JH, Digumarthy SR, et al. Common and uncommon manifestations of Wegener granulomatosis at chest CT: radiologic-pathologic correlation. Radiographics **32**: 51-69, 2012.

14. Hur JH, Chun EJ, Kwag HJ, et al. CT features of vasculitides based on the 2012 International Chapel Hill Consensus Conference revised classification. Korean J Radiol **18**: 786-798, 2017.

15. Anderson RH, Mori S, Spicer DE, Sanchez-Quintana D, Jensen B. The anatomy, development, and evolution of the atrioventricular conduction axis. J Cardiovasc Dev Dis **5**: E44, 2018.